Ultraviolet fluorescence detection and identification of protein, dna, and bacteria

P. J. Hargis, Jr., T. J. Sobering, G. C. Tisone, and J. S. Wagner

Sandia National Laboratories
Albuquerque, New Mexico 87185

S. A. Young and R. J. Radloff

University of New Mexico School of Medicine, Department of Microbiology
Albuquerque, New Mexico

ABSTRACT

Recent food poisoning incidents have highlighted the need for inexpensive instrumentation that can detect food pathogens. Instrumentation that detects the relatively strong ultraviolet (UV) fluorescence signal from the aromatic protein amino acids in bacteria could provide a solution to the problem of real-time pathogen measurements. The capabilities of UV fluorescence measurements have, however, been largely ignored because of the difficulty in identifying pathogens in the presence of interfering backgrounds. Implementation of fluorescence measurements thus requires methodologies that can distinguish fluorescence features associated with pathogens from those associated with proteins, harmless bacteria, skin, blood, hair follicles, pesticide residue, etc. We describe multispectral UV fluorescence measurements that demonstrate the feasibility of detecting and identifying protein, DNA, and bacteria using a relatively simple UV imaging fluorometer and a unique multivariate analysis algorithm.

2. INTRODUCTION

Advances in remote sensing technologies, including high-speed computing and new photodetectors, are permitting electro-optic sensing to address needs that were previously impractical due to cost and complexity issues. Food Safety is one such area where the need for improved sensors exists, but low profit margins preclude the use of most advanced technologies. Outbreaks of food poisoning associated with *E. coli* O157:H7 have highlighted the need for inexpensive instrumentation to provide rapid, automated detection of food pathogens during the preparation and processing of foods.

Sandia National Laboratories has a long history of applying spectroscopic and laser remote sensing techniques to the detection of airborne pollutants in the laboratory and the atmosphere. Our development of multivariate analysis algorithms for the detection and identification of pollutants through their ultraviolet fluorescence signatures has resulted in significant improvements in sensitivity, particularly in the presence of contaminating background signatures. It is believed that this work can be scaled to be directly applicable to the near real-time detection of food pathogens in the laboratory or during the processing, handling, and packaging of food and food products. It is recognized that bacteria exhibit strong fluorescence spectra when excited by an external ultraviolet source. What is currently not known, however, is 1) whether these signatures are sufficiently unique to permit a practical, inexpensive detection system to be developed based on UV fluorescence spectroscopy, and 2) whether the measurement sensitivity of such a system is high enough to reliably reduce the risk to the consumer. This paper discusses exploratory measurements that demonstrate the feasibility of applying multispectral UV fluorescence spectroscopy and multivariate processing algorithms to the detection and classification of protein, DNA, and *E. coli* (ATCC 25922).

3. MULTISPECTRAL ULTRAVIOLET FLUORESCENCE

Measurements at Sandia have demonstrated that UV measurements can detect a wide variety of airborne pollutants that absorb optical radiation in the 250 to 400 nm wavelength range.[1] As shown in Fig. 1, typical UV absorption spectra for airborne pollutants are broad and relatively featureless in comparison to similar spectra in the infrared. In addition, UV absorption spectra from different pollutants overlap each other. As a result, light at, for example, 250 nm is absorbed by all six

0-8194-1712-2/95/$6.00

pollutants shown in Fig 1. Similar spectral overlap and congestion also occurs in UV fluorescence spectra. This is illustrated in Fig. 2 by the fluorescence spectrum from a mixture of acetone, benzene, methanol, toluene, and xylene in relative volumetric concentrations of 1:1:1:1:1:0.01, respectively. The spectrum in Fig. 2 is a dispersed fluorescence excitation spectrum, sometimes called the total fluorescence spectrum. The low-resolution fluorometer shown in Fig. 3 was used to measure the fluorescence spectrum in Fig. 2. The spectrum was obtained by sequentially scanning the wavelength of the xenon arc lamp from 200 to 400 nm in 5 nm steps. At each excitation wavelength, the dispersed fluorescence spectrum was recorded with the diode array detector. The data in Fig. 2 thus consists of a series of 41 discrete dispersed fluorescence spectra. Peaks and valleys in the spectrum correspond to peaks and valleys in the absorption and fluorescence spectrum of each chemical component in the mixture. Also evident in Fig. 2 are relatively narrow first and second order spectral peaks corresponding to scattered light from the xenon arc lamp. As shown below, similar spectra are obtained for protein, DNA, and *E. coli*.

3.1. Background

Spectroscopic measurements based on differential light scattering[2], visible and near-infrared reflectance[3], and laser Raman spectroscopy[4] have been used to detect bacteria. In general, these spectroscopic techniques are either too complex, too expensive, or too insensitive to be used for real-time pathogen measurements. Instrumentation that detects the relatively strong UV fluorescence signal from the aromatic protein amino acids in the cell walls of bacteria could provide an inexpensive solution to the problem of real-time pathogen measurements. Practical implementation of such instrumentation, however, requires measurement methodologies that can distinguish fluorescence features associated with food pathogens from those associated with proteins, harmless bacteria, skin, blood, hair follicles, pesticide residue, etc. Other research groups have largely ignored the capabilities of UV fluorescence measurements in the identification of food pathogens because of the difficulty in detecting and identifying pathogens in the presence of the expected complex backgrounds. Our development of a unique multivariate analysis algorithm[5] that excels at unraveling individual spectra from multispectral UV fluorescence measurements, such as those shown in Fig. 2, gives us a unique perspective on the capabilities of UV fluorescence measurements. The algorithm, as originally developed, has a demonstrated capability to identify trace concentrations of organic chemical species in mixtures of chemicals.[5] Application of the algorithm to the data in Fig. 2 has shown, for example, that UV fluorescence measurements can identify as little as 10 ppm xylene in mixtures of acetone, benzene, methanol, and toluene. The challenge in our work on pathogen detection is to optimize the existing algorithm to distinguish pathogens from harmless bacteria and other contaminants. As a first step, exploratory measurements were carried out in collaboration with the University of New Mexico to determine the ability of UV fluorescence measurements to detect and distinguish protein, DNA, and *E. coli*..

3.2. Exploratory Measurements

Four examples of multispectral UV fluorescence spectra are included as examples of the type of data obtained with the low-resolution (5 nm FWHM bandwidth) UV fluorometer shown in Fig. 3. Each example shows the uncorrected data obtained from the fluorometer as well as a contour plot of the total fluorescence spectrum. The x-axis corresponds to the fluorescence wavelength and the y-axis to the excitation wavelength. Data were obtained by scanning the excitation wavelength from 200 nm to 400 nm in 5 nm steps and measuring the dispersed fluorescence spectrum at each excitation wavelength with an intensified diode array having single-photon detection sensitivity. The active region of the fluorescence spectrum extends from ~200 nm to ~400 nm. A typical spectrum was obtained in 2 to 10 min. The first example, Figure 4, shows the multispectral UV fluorescence spectrum from 10 ppm bovine serum albumin (BSA) in a phosphate buffered saline (PBS) solution. The second example, Figure 5, shows a the fluorescence spectrum from 100 ppm calf thymus DNA in PBS. Careful examination of the fluorescence contours shows a distinct offset between the centroids of the DNA and BSA fluorescence peaks. Figure 6 is an interesting example illustrating the sensitivity of multispectral UV fluorescence measurements to impurities. The fluorescence spectrum in Figure 6 was obtained from 10 ppm calf thymus DNA in PBS. At least 5 impurity peaks, which completely mask the DNA fluorescence peaks, are evident in Figure 6. The final example, Figure 7, shows the fluorescence spectrum from *E. coli* (ATCC 25922). Again, careful inspection of the fluorescence contours shows distinct offsets between the *E. coli* fluorescence bands and those of DNA and BSA. Also evident in Figure 7 is a weak PBS Raman band. Fluorescence signal intensities were linear over a three order of magnitude change in the concentration of BSA, DNA, and *E. coli* in PBS. In addition, fluorescence lineshapes did not change over the same concentration range. The distinct offsets

in the fluorescence contours from BSA, DNA, and *E. coli* give us confidence in the ability of multivariate algorithms to distinguish protein, DNA, and bacteria.

3.3. Multivariate analysis

Multivariate analysis algorithms developed to identify chemical components in multispectral UV fluorescence spectra from multicomponent samples were used to analyze the fluorescence spectra shown in Figs. 4, 5, and 7.[5] The spectra were added to a database of approximately 20 spectra from potential aromatic interferents such as benzene, toluene, xylene, gasoline, etc. Even though the algorithm was not trained to recognize spectral signatures from BSA, DNA, and *E. coli*, it was still able to correctly identify BSA, DNA, and *E. coli* using the spectral database. In some cases, however, the algorithm had trouble identifying DNA concentrations below 10 ppm, confusing it with BSA and *E. coli*. Proper training of the algorithm using the procedures outlined in Ref. 5 should alleviate this confusion.

4. SUMMARY

Exploratory multispectral UV fluorescence measurements made on bovine serum albumin, calf thymus DNA, and *E. coli* (ATCC 29522) have demonstrated that multivariate analysis algorithms can distinguish protein, DNA and bacteria fluorescence signatures from interfering backgrounds. Future results will address the effect of measurement and growth environments on the reproducibility of the measurements as well as determine multispectral fluorescence signatures of pathogenic bacteria.

5. ACKNOWLEDGMENTS

We would like to acknowledge Ben Aragon for his contributions to the design of the UV fluorometer used in the exploratory measurements. Work performed at Sandia National Laboratories was supported by the United States Department of Energy under Contract DE-AC04-94AL85000.

6. REFERENCES

1. P. J. Hargis, Jr., G. C. Tisone, J. S. Wagner, M. W. Trahan, A. V. Smith, T. D. Raymond, W. J. Alford, G. N. Hays, A. B. Wegner, J. E. M. Goldsmith, M. Lapp, and S. E. Bisson, "Multispectral Ultraviolet Fluorescence Lidar Detection of Volatile Compounds in the Atmosphere", in *Optical Sensing for Environmental Monitoring*, Proceedings of the 1993 Air & Waste Management Association Conference, Atlanta, Georgia, October 11-14, 1993, Air & Waste Management Association, Pittsburgh, p. 756, 1993.

2. B. V. Bronk, W. P. Van de Merwe, and M. Stanley, "In Vivo Measure of Average Bacterial Cell Size from a Polarized Light Scattering Function", Cytometry **13**, p. 155, 1992.

3. Y. R. Chen, "Classifying Diseased Poultry Carcasses by Visible and Near-IR Reflectance Spectroscopy, in *Optics in Agriculture and Forestry*, SPIE Vol. 1836, p. 46, 1992.

4. W. H. Nelson, R. Manoharan, and J. F. Sperry, "UV Resonance Raman Studies of Bacteria", Appl. Spectrosc. Rev. **27**, p. 67, 1992.

5. J. S. Wagner, M. W. Trahan, W. E. Nelson, P. J. Hargis, Jr., and G. C. Tisone, "Chemical Recognition Software", to be published in *Optical Sensing for Environmental and Process Monitoring*, Proceedings of the 1994 Air & Waste Management Association Conference, McLean, Virginia, November 7-10, 1994.

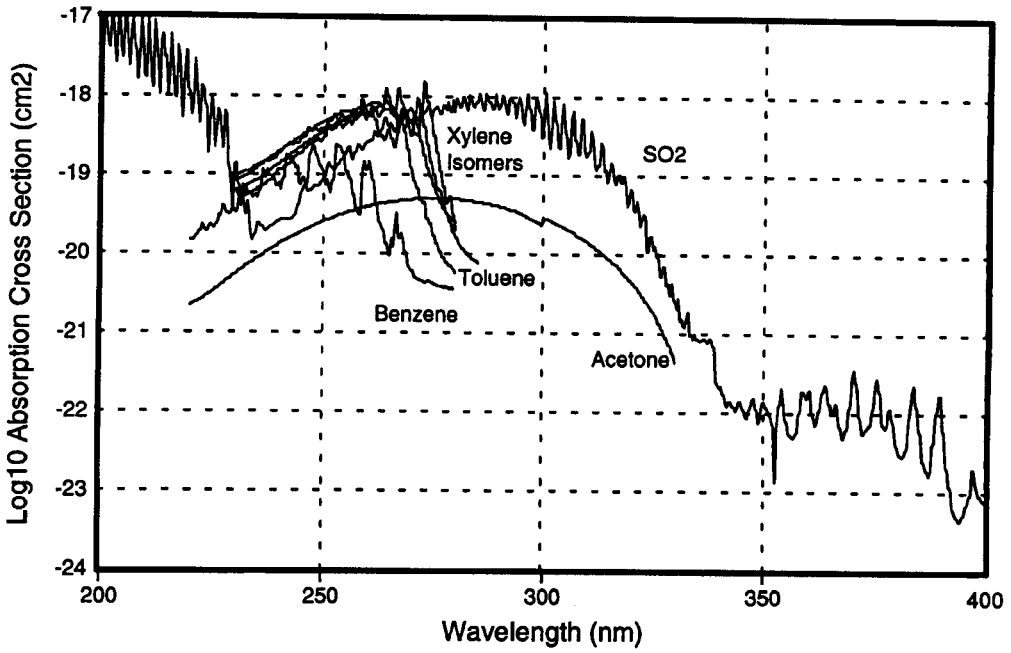

Figure 1. Absorption cross sections for acetone, benzene, SO_2, toluene, and the xylene isomers.

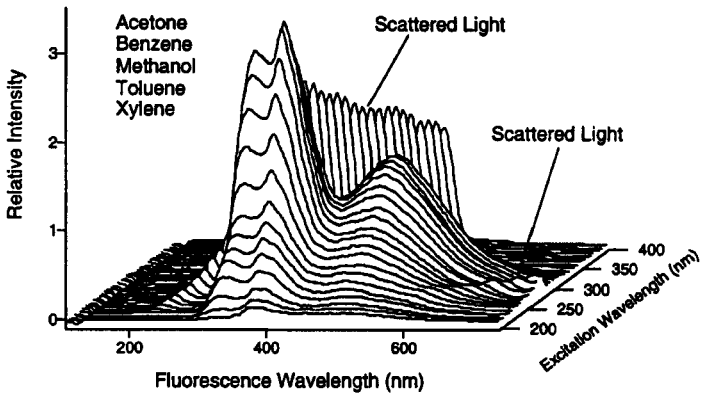

Figure 2. Total fluorescence spectrum from a mixture of acetone, benzene, methanol, toluene, and xylene.

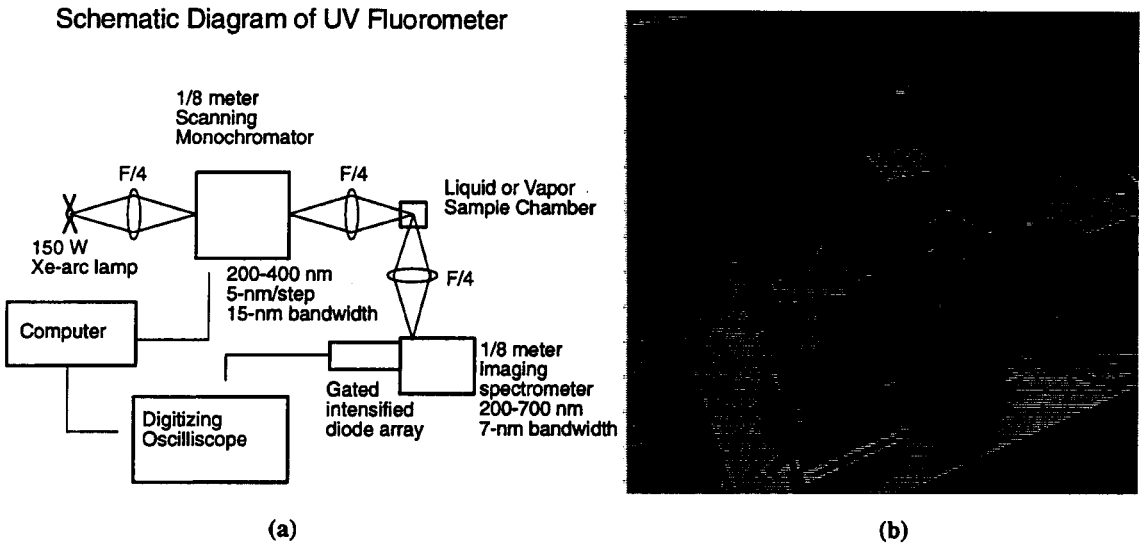

(a) (b)

Figure 3. Schematic diagram (a) and photograph (b) of the low-resolution UV fluorometer used for total fluorescence measurements.

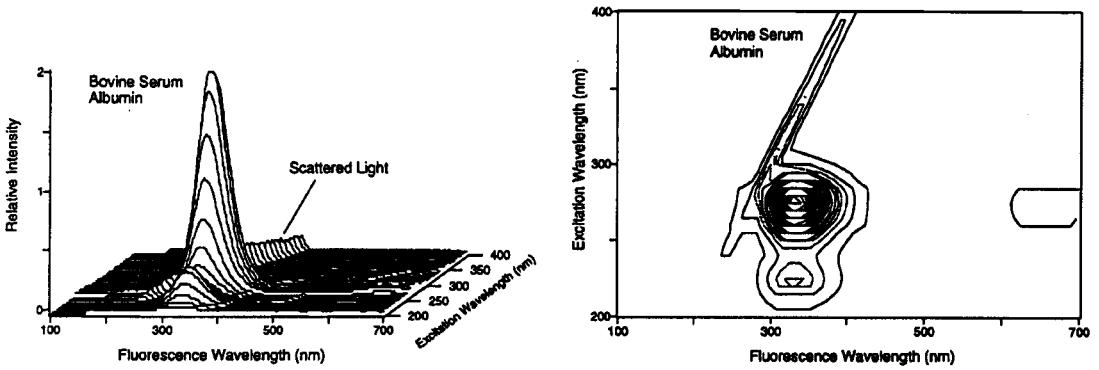

(a) (b)

Figure 4. Total fluorescence spectrum (a) and contour map (b) of 10 ppm bovine serum albumin in a phosphate buffered saline solution. The two fluorescence peaks evident in the contour map occur at a fluorescence wavelength of 330.7 nm and excitation wavelengths of 222.5 nm and 276.9 nm.

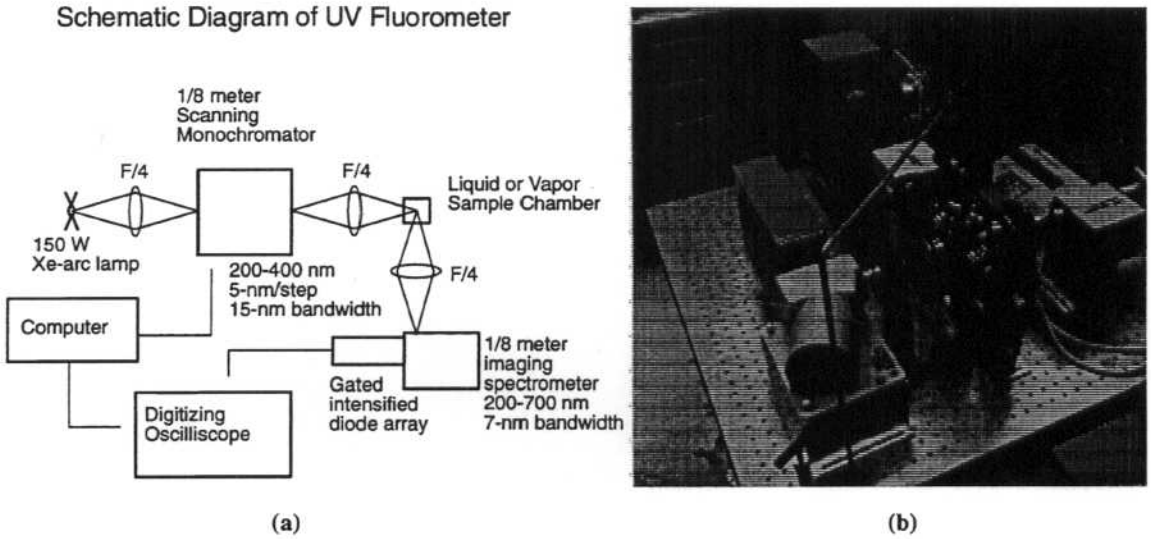

Figure 3. Schematic diagram (a) and photograph (b) of the low-resolution UV fluorometer used for total fluorescence measurements.

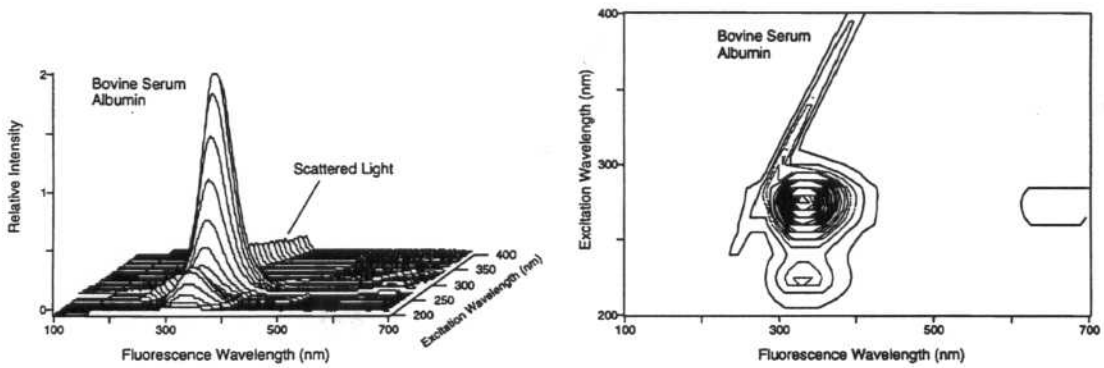

Figure 4. Total fluorescence spectrum (a) and contour map (b) of 10 ppm bovine serum albumin in a phosphate buffered saline solution. The two fluorescence peaks evident in the contour map occur at a fluorescence wavelength of 330.7 nm and excitation wavelengths of 222.5 nm and 276.9 nm.

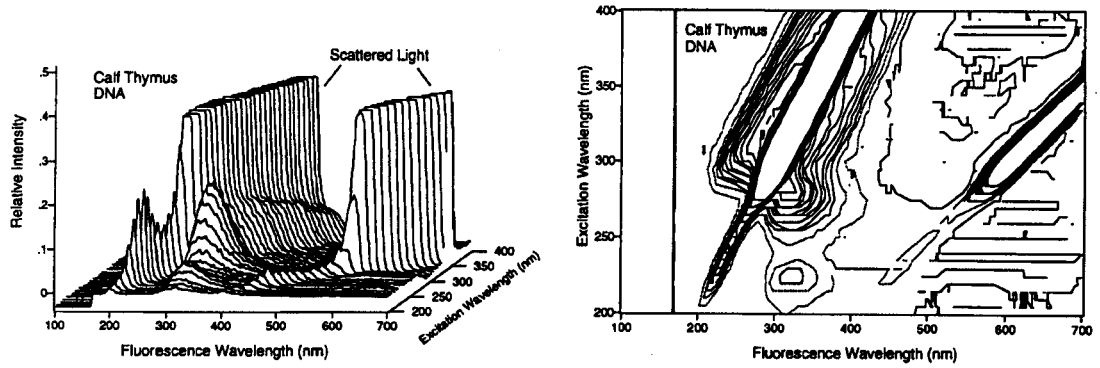

(a) (b)

Figure 5. Total fluorescence spectrum (a) and contour map (b) of 100 ppm calf thymus dna in a phosphate buffered saline solution. The two fluorescence peaks evident in the contour map occur at a fluorescence wavelength of 321.6 nm and excitation wavelengths of 224.3 nm and 280.6 nm.

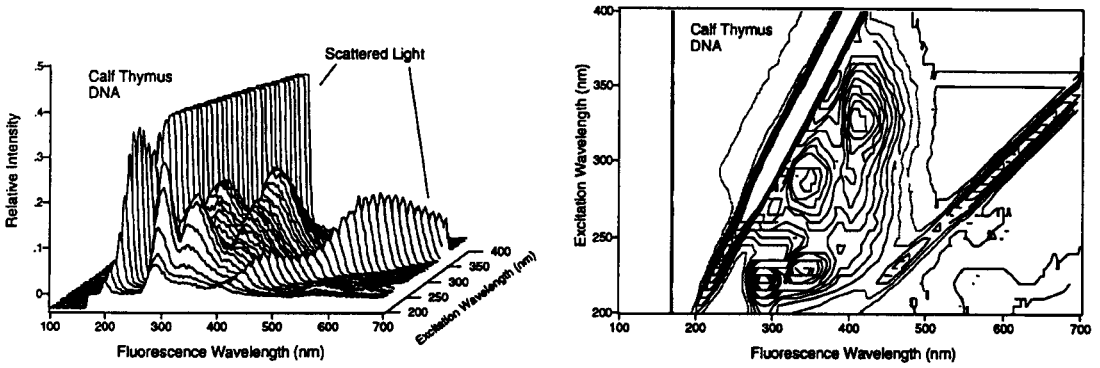

(a) (b)

Figure 6. Total fluorescence spectrum (a) and contour map (b) of 10 ppm calf thymus dna in a contaminated phosphate buffered saline solution. The fluorescence spectrum is dominated by impurities which completely mask the calf thymus dna spectrum. At least 5 impurity peaks are evident in the contour map.

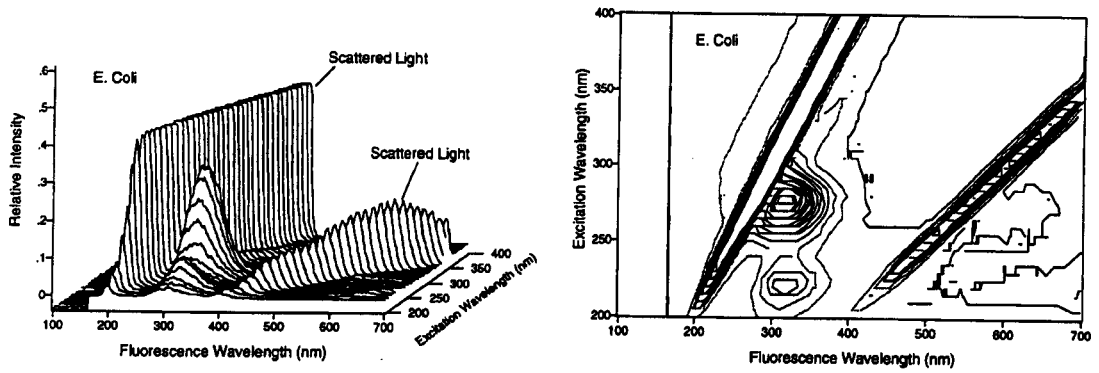

(a) (b)

Figure 7. Total fluorescence spectrum (a) and contour map (b) of *E. coli* (ATCC 25922) in a phosphate buffered saline solution. The estimated *E. coli* concentration ranges from 10^3 to 10^4 organisms/cm^3. The two fluorescence peaks evident in the contour map occur at a fluorescence wavelength of 317.7 nm and excitation wavelengths of 220.6 nm and 277.5 nm.